



HAL
open science

Reproducibility of High Resolution Optical Coherence Tomography Measurements of the Nerve Fiber Layer with the new Heidelberg Spectralis OCT

Nermin Serbecic, Sven C Beutelspacher, Fahmy Aboul-Enein, Karl Kircher, Andreas Reitner, Ursula Schmidt-Erfurth

► **To cite this version:**

Nermin Serbecic, Sven C Beutelspacher, Fahmy Aboul-Enein, Karl Kircher, Andreas Reitner, et al.. Reproducibility of High Resolution Optical Coherence Tomography Measurements of the Nerve Fiber Layer with the new Heidelberg Spectralis OCT. *British Journal of Ophthalmology*, 2010, 95 (6), pp.804. 10.1136/bjo.2010.186221 . hal-00595937

HAL Id: hal-00595937

<https://hal.science/hal-00595937>

Submitted on 26 May 2011

HAL is a multi-disciplinary open access archive for the deposit and dissemination of scientific research documents, whether they are published or not. The documents may come from teaching and research institutions in France or abroad, or from public or private research centers.

L'archive ouverte pluridisciplinaire **HAL**, est destinée au dépôt et à la diffusion de documents scientifiques de niveau recherche, publiés ou non, émanant des établissements d'enseignement et de recherche français ou étrangers, des laboratoires publics ou privés.

Reproducibility of High Resolution Optical Coherence Tomography Measurements of the Nerve Fiber Layer with the new Heidelberg Spectralis OCT

N. Serbecic^{1*}, S.C. Beutelspacher¹, F.C. Aboul-Enein², K. Kircher¹, A. Reitner¹ and U. Schmidt-Erfurth¹

1. Medical University of Vienna, Department of Ophthalmology, Vienna, Austria

2. SMZ-Ost, Donauspital, Department of Neurology, Vienna, Austria

Corresponding Author:

Dr. Nermin Serbecic
Medical University of Vienna
Department of Ophthalmology
Vienna, Austria
Tel. +43-1-40400-7930
Fax +49-1-40400-7932
Mail nermin.serbecic@meduniwien.ac.at

Keywords: optical coherence tomography, retinal nerve fiber layer, axonal degeneration, reproducibility

Word Count: 3070

NS and SCB have equally contributed to this manuscript.

Licence for Publication

The Corresponding Author has the right to grant on behalf of

all authors and does grant on behalf of all authors, an exclusive licence (or non exclusive for government employees) on a worldwide basis to the BMJ Publishing Group Ltd to permit this article (if accepted) to be published in BJO and any other BMJ PGL products and sublicences such use and exploit all subsidiary rights, as set out in our licence (<http://group.bmj.com/products/journals/instructions-for-authors/licence-forms>).

Competing Interest: None to declare.

Abstract

Purpose

Conventional time-domain OCT technology for detection of retinal nerve fiber layer (RNFL) neurodegeneration suffers from technical inaccuracy due to a lack of exact scan centering around the optic disc as well as a true follow-up possibility. In this study, we evaluated a novel high-resolution Spectral-domain OCT device (SD-OCT) with an incorporated eye-tracking feature in its ability to objectively measure the RNFL thickness (RNFLT) by testing intra-observer reproducibility in a series of healthy volunteers.

Methods

Triplicate circumferential RNFL scans of six peripapillary sectors were obtained from both eyes of all 31 participants. We compared the measurements of RNFLT during three separate examination days under miotic (Mi) and mydriatic (My) pupil conditions using high-speed (HS) and high-resolution (HR) scan acquisition mode. To examine the intersession reproducibility of the SD-OCT measurements the mean, standard deviation and the coefficient of variation (COV) were calculated

Results

No significant differences were found in all groups, independent of the mode of image acquisition and examination day (p always $> 0,05$). Under all conditions, low coefficients of variation (COV) between 0.545% and 3.97% (intrasession COV on baseline) were found. The intersession COV with activated follow-up mode ranged between 0.29% and 1.07%. In both settings the temporal sector showed the highest COV values.

Conclusions

True follow-up measurement of identical peripapillary regions may enable clinicians to detect discrete levels of retinal thickness change over time. This constitutes a crucial prerequisite for a reliable monitoring of subtle RNFL changes in neurodegenerative disorders.

Introduction

Previous studies have almost exclusively used standard time-domain optical coherence tomography (TD-OCT, **Stratus OCT; Carl Zeiss Meditec, Dublin, California, USA**) as a non-invasive retinal ocular imaging technique to measure structural changes in the axonal integrity of the retinal nerve fiber layer (RNFL) in patients with glaucoma, various optic neuropathies, optic neuritis (ON) and/or multiple sclerosis (MS).**[1-3]** In most of the MS cases, the discrete progressive axonal changes may be elusive during short monitoring but may become more obvious in long observation periods. [4, 5]

Before OCT technology can be widely accepted for use in monitoring subtle axonal loss, often interpreted as a sign of progression of neurodegenerative diseases, it is **however** important that its initial diagnostic accuracy on baseline **examinations** can be extended to reproducible comparisons of retinal nerve fiber layer thickness (RNFLT) over time. To describe the smallest changes detectable in the context of a rather complex CNS disease, the latest advances in OCT technology have led to the incorporation of high-resolution spectral-domain (SD-OCT) imaging. **This technique offers** significant advantages in terms of markedly improved image resolution, imaging speed, scan coverage and retinal segmentation algorithms over the conventional TD-OCT.**[6]** Accordingly, **in overcoming** the problems of prolonged examination time and difficulties in scan centering around the optic disc due to poor fixation **and eye movements (in visually impaired or disabled patients)** this latest SD-OCT **technology provides novel technological features.**

For instance, the SD-OCT device offers a unique feature **of "freezing" the** retinal infrared **fundus image, utilizing** a real time averaging algorithm. For this purpose the OCT scan can be moved within this **stabilized** optic disc image, **so as to optimize** exact scan centering. **In conjunction with a built-in eye-tracking mechanism [7, 8] image artifacts due to eye movements are consequently ruled out. Additionally, the OCT software can automatically identify previous scan locations and "guide" the OCT broadband light source to scan the same location repeatedly and observer independently during follow-**

up visits. As a result, the technology markedly facilitates an objective and quantitative evaluation of the RNFLT over time.

We have assessed the ability of the new SD-OCT device to objectively measure RNFL thickness by testing intra- and intersession variability globally around the optic disc and also in the temporal, superior, nasal and inferior peripapillary sectors in a series of healthy volunteers as follows: 1) a comparison of the detection of RNFLT in dilated and undilated eyes either using high-speed (HS) or high-resolution (HR) image acquisition mode; 2) a comparison of examinations of the RNFLT with either repeatedly activated automated real-time averaging mode (ART-Mode) and repositioning of the OCT scan target area over the optic disc for each scan or continuously activated ART mode during measurements with locked target area over the fixed optic disc reference fundus image for several image scans; 3) a comparison of automatic RNFLT detection in the follow-up mode using a baseline examination and two consecutive measurements on different days.

Materials and Methods

Patients

62 eyes of 31 healthy subjects (mean age female: 33±11,27 years; mean age male 31±6,29) were included into the study. The inclusion criteria for all participants were a best-corrected visual acuity of 20/40 or better, a spherical refraction within ±5.0 diopters (D), cylinder correction within ±2.0 diopters and normal results on Humphrey visual field testing. Exclusion criteria were the presence of media opacifications, a history of ocular surgery, trauma or ocular diseases affecting the cornea, lens, retina, or optic nerve. The intraocular pressure (IOP) measured with Goldmann applanation tonometry was between 11 mmHg and 21 mmHg. All subjects received a slit-lamp exam and dilated fundus examination prior to inclusion. Informed consent was obtained from all participants.

RNFL Measurement

Heidelberg Spectralis Optical Coherence tomography (SD-OCT) (Heidelberg Engineering, Heidelberg, Germany, Spectralis software version 5.1.1.0, Eye Explorer Software 1.6.1.0) uses a scanning superluminescence diode to emit a scan beam with a wavelength of 870 nm to provide up to 40,000 A scans/sec with a depth resolution of 7µm in tissue and a transversal resolution of 14 µm of images of ocular microstructures. The instrument combines OCT technology with a confocal Scanning Laser Ophthalmoscope (Heidelberg Engineering, Heidelberg, Germany), which provides a reference infrared fundus image.

An internal nasal fixation light was used to center the disc in the incorporated circle-shaped scanning target area. For OCT scanning, the SD-OCT device offers a unique feature of "freezing" the retinal infrared fundus image, utilizing a real time averaging algorithm (ART-mode). For this purpose the OCT scan can be moved within this stabilized optic disc image, so as to optimize exact scan centering and to adjust the number of obtained frames (=B scans, of which a number of 1-16 frames can be chosen for each peripapillary scan) to average

and enhance image quality for each image scan. In the study, this was achieved using a maximum of 16 frames for each scan of the same scanning location during the peripapillary scanning process, thereby optimizing the signal to noise ratio and image quality significantly. Additionally, the device includes a high-speed (HS) and also a high-resolution (HR) mode for the OCT scan acquisition. First, the HS mode allows fast image acquisition; however, the images appear in lower resolution, yet still sufficient for automated layer segmentation. Second, the more time-consuming HR mode delivers high-resolution image quality scans with a clear visualization of each retinal layer. Furthermore, signal strength has been shown to affect RNFLT measurements using conventional Stratus OCT [9, 10]. Therefore, in cases where the OCT software failed to detect the nerve fiber layer due to low image quality (failed automatic segmentation), obtained scans were eliminated and measurements were repeated until excellent quality was achieved. Although a manual correction of the segmentation is provided by the manufacturer, none was performed. Criteria for determining scan quality include a clear fundus image allowing perfect optic disc and scan circle visibility before and during image acquisition, absence of scan or algorithm errors which correspond to a signal strength of 20 units (as shown by the internal signal strength control) or more as suggested by the manufacturer, even and dense grey scale saturation throughout all retinal layers with dense grey visible in the RPE, and the RNFL visible with no irregularities and a continuous scan pattern. The OCT RNFLT scans were performed several times by a single operator (N.S.) during one individual session until at least three high-quality scans were obtained and used for further analysis. Scans were acquired in the high-resolution acquisition mode thus allowing a more detailed differentiation of retinal layers, and in the high-speed mode for faster acquisition, but lower image quality, both in miosis followed by a series of scans in mydriasis (Figure 3 B and C). By means of eye tracking (TrueTrac™), each peripapillary OCT scan is registered and locked to a reference image utilized by the ART-mode. The built-in eye tracking modality and the high scanning speed are supposed to reduce image artifacts due to eye movements. In addition, the OCT software can identify

previous scan locations (follow-up mode) and "guide" the OCT broadband light source to scan the same location repeatedly during follow-up visits.

In our study, triplicate image scans were obtained within a single session in all eyes for baseline as well as follow-up visits. For each of the three OCT scans, the maximum number of 16 frames, either in HR or HS mode, was utilized. To assess the reproducibility of SD-OCT measurements of the RNFLT we compared a specific set of different OCT scan acquisition modes.

In a first step (corresponding to baseline examination), we addressed the question of whether individuals with clear optic media, dilation of the pupil would be necessary. In addition, we analyzed whether the high resolution (HR) mode would deliver more accurate results than the high speed (HS) mode. Moreover, we performed measurements in repeatedly activated ART-mode (automated real-time averaging mode, either as HS- or HR-mode) with more time-consuming manual disc centering in the scanning area for each of the three peripapillary RNFL measurements. Furthermore, we examined in the same session with continuous ART-mode (either as HS-A- or HR-A-mode) utilizing permanently activated automated real-time averaging during measurements with locked target area over the fixed optic disc reference fundus image for several scans, whilst to avoid detection of the same image reacquisition of 16 frames each time (Figure 2 & 3). These settings were, in all cases, evaluated circumferentially and individually in the temporal, inferior, nasal and superior peripapillary sectors.

In a second step (corresponding to the performed two follow-up visits and based on the results of the baseline examinations), triplicate scans (each scan with the maximum number of 16 frames) for each session, again in the HR,- and HS-modes, were performed in miosis and mydriasis to evaluate intersession variability.

Statistical Analysis

In all cases triplicate high-quality scans were acquired. In

the case of the baseline examination, each of the three obtained scans consisted of the maximum achievable number of 16 averaged frames.

The different groups were plotted as box-plots, representing the different image acquisition modes. They were compared a paired, two-tailed t-test, taking a $p \leq 0,05$ as statistically significant. The standard deviation was calculated as the square root of the variance. Reproducibility was assessed by calculating the coefficient of variation (COV) for intravisit and intervisit measurements. The intrasession COV (within-subject variability) was calculated by dividing the square-root of the within-visit variance component by the average of the measurements and was expressed as a percentage, with a COV < 5% expressing a good reproducibility. As a measure of intersession reproducibility (representing the expected amount of long term variability) we calculated the COV (%) over the parameter values (standard deviation / COVs) in the base, F1 and F2 session as the overall standard deviation (base, F1 and F2) divided by the average.

Results

1.) Baseline examination: comparison of RNFLT measurements in dilated and undilated eyes

In the circumferential frame, we found slightly higher values for the RNFLT in dilated versus undilated eyes, however, without noting statistical significance (Table 1, $p > 0.05$). The measurements (all μm) of the RNFLT were in a range of 97.95 ± 0.64 (undilated, Mi-HR-A-mode) and 101.34 ± 0.685 (dilated, My-HR-A-mode). In the temporal quadrant, we found values between 72.77 ± 2.095 (dilated, My-HR-A-mode) and 76.45 ± 2.985 (dilated, My-HR-mode). Inferiorly, we detected thickness values for the RNFLT in a range between 123.11 ± 1.545 (undilated, Mi-HS-A-mode) and 125.46 ± 2.715 (undilated, Mi-HR-mode). In the nasal quadrant, RNFLT thickness ranged between 75.975 ± 2.26 (undilated, HR-A-mode) and 79.37 ± 2.22 (undilated, Mi-HR-mode). In the superior quadrant, the measurements for RNFLT thickness were between 121.43 ± 2.93 (undilated, Mi-HR-A-mode) and 124.94 ± 2.85 (dilated, My-HR-A-mode). In all cases no statistical significance was found within the different sectors (p always $> 0,05$).

To examine the intergroup variability (regarding the different image acquisition modes) of the Spectralis OCT measurements, the mean, standard deviation and the coefficient of variation (COV) were determined under different conditions as described previously (miosis high resolution (=Mi-HR), miosis high resolution with locked ART mode (=Mi-HR-A), miosis high speed (=Mi-HS), miosis high speed with locked ART mode (=Mi-HS-A), mydriasis high resolution (=My-HR), mydriasis high resolution with locked ART mode (=My-HR-A), mydriasis high speed (=My-HS), mydriasis high speed with locked ART mode (=My-HS-A)) in all peripapillary sectors (global = G, temporal = temp, inferior = inf, nasal = nas, superior = sup). The results are demonstrated in Table 1. Under all conditions, low intrasession coefficients of variation (COV) between 0.545% (G My-HS-A) and 3.97% (temp My-HR) were found. The lowest intrasession COV was documented in the global (G) RNFLT measurement ranging between 0,545% (My-HS-A) and 1.72% (My-HR). Interestingly, the highest COVs were detected in the

temporal sector ranging between 2.71% (Mi-HS-A) and 3.97% (My-HR).

		G	temp	Inf	nas	sup
Mi HR	Mean	99,725	75,25	125,46	79,365	123,33
	Stdev	1,565	2,605	2,715	2,215	3,07
	COV (%)	1,555	3,46	2,185	3,055	2,485
Mi HR-A	Mean	97,95	75,255	123,73	75,975	121,43
	Stdev	0,64	2,26	1,8	2,255	2,925
	COV (%)	0,655	3,08	1,445	3,19	2,435
Mi HS	Mean	98,59	73,63	124,00	78,78	122,82
	Stdev	1,17	2,54	2,065	1,985	2,48
	COV (%)	1,195	3,465	1,67	2,755	2,05
Mi HS-A	Mean	98,02	73,29	123,11	78,25	121,90
	Stdev	0,76	1,96	1,545	1,55	1,835
	COV (%)	0,58	2,71	1,285	2,14	1,535
My HR	Mean	100,305	76,445	125,235	79,19	124,84
	Stdev	1,75	2,985	3,635	2,065	3,48
	COV (%)	1,72	3,97	2,87	2,82	2,825
My HR-A	Mean	101,34	72,77	124,58	78,03	124,94
	Stdev	0,685	2,095	2,49	2,145	2,845
	COV (%)	0,67	2,85	1,955	3,06	2,24
My HS	Mean	99,02	74,28	123,75	78,35	124,09
	Stdev	1,5	2,56	2,19	2,52	2,49
	COV (%)	1,505	3,47	1,785	3,42	1,97
My HS-A	Mean	98,91	74,49	123,83	78,22	123,66
	Stdev	0,535	2,36	1,815	1,99	1,73
	COV (%)	0,545	3,28	1,475	2,785	1,375

Table 1

2.) Follow-up RNFLT measurements: Comparison of RNFLT in dilated and undilated eyes over 3 different days.

Having discerned that there are no measuring differences between dilated and undilated eyes on baseline (irrespective of the image acquisition mode), we proceeded to investigate whether the measurements of the RNFLT would be reproducible over time, i.e. during three separate days (Table 2). This task was undertaken using the "baseline / follow-up" setting of the Spectralis device. (Technical explanation: once an obtained image scan is marked as a baseline examination scan, subsequent examinations and OCT scans can be taken at identical positions using the built-in follow-up mode, which is utilised by a second, detecting laser source.) Accordingly, we compared the high-speed with the high-resolution mode.

We used Box-Plots to compare the RNFLT values between the different examination days (base/F1/F2) and modes (HR/HS) (Figure 1). Again, no significant differences were found between the different groups. In none of the sectors analyzed were significant differences in direct comparison found ($p > 0.05$). The comparison of the same parameters in dilated eyes again showed no statistically significant differences (data not shown, p in all cases $> 0,05$).

We then examined the intersession variability of the Spectralis OCT measurements in regard to the baseline examination and two consecutive examinations under identical conditions on the two following days (F1 and F2). Again, we calculated the mean, standard deviation and the coefficient of variation (COV) using the different conditions described previously. The results are shown in table 2. COV ranged between 0,29% (sup, Mi-HS) and 1,07% (temp, Mi-HS). In dilated eyes, the COV was ranging between 0,35 (sup, My-HS) and 1,12 (temp, My-HS).

Table 2

<i>Miosis</i>	<i>G</i>	<i>Temp</i>	<i>Inf</i>	<i>Nas</i>	<i>Sup</i>
HR					
Mean (μm)	96,73	73,68	117,04	78,42	118,93
Stdev	0,41	0,655	0,63	0,62	0,41
COV (%)	0,42	0,885	0,525	0,855	0,535
HS					
Mean	95,25	73,285	117,54	77,765	116,935
Stdev	0,29	0,78	0,37	0,63	0,34
COV (%)	0,31	1,07	0,315	0,895	0,29

<i>Mydr.</i>	<i>G</i>	<i>Temp</i>	<i>Inf</i>	<i>Nas</i>	<i>Sup</i>
HR					
Mean (μm)	97,43	75,25	120,06	77,24	118,96
Stdev	0,05	0,81	0,82	0,73	0,42
COV (%)	0,53	1,02	0,64	0,95	0,55
HS					
Mean	95,99	74,39	118,85	78,31	117,83
Stdev	0,58	0,90	0,29	0,685	0,49
COV (%)	0,49	1,12	0,45	0,85	0,35

Discussion

Among neuroophthalmologists and neurologists who care for MS patients, conventional TD-OCT technology is currently being discussed both as a means of monitoring the progression of the disease and in evaluating the impact of disease-modifying therapy.[11]

However, the reproducibility of RNFLT measurements is crucial for its diagnostic precision if the application of OCT is expected to evolve into a reliable outcome metric for the efficacy of longitudinal clinical trials. It should be used to precisely monitor disease course in terms of slowly progressive subtle axonal loss thereby reflecting the degenerative processes in the central nervous system. [12] In fact, RNFLT anatomically increases as proximity to the optic disc increases.[13] Consequently, even a minimal decentering of the target will lead to significantly differing results in RNFLT measurements obtained by TD-OCT.[14] An adequate OCT resolution and optimized image quality already at baseline are therefore of paramount concern in patients suffering from optic nerve- and neurodegenerative disorders.

Poor fixation - resulting from (ceco-) central scotomas, nystagmus, macular degeneration or progressive optic neuropathy - may be challenging during scan acquisition. For example, with conventional TD-OCT, reproducible RNFL scans during episodes of acute optic neuritis can hardly be achieved [13]. The current study provides evidence that SD-OCT technology, by incorporating an eye-tracking mode, has the potential to accurately and repeatedly perform RNFLT measurements. For the first time, fixation problems can be overcome using the eye tracking option. As opposed to conventional TD-OCT-devices [14] a circle-shaped central target area is incorporated. It can be positioned directly on the rim of the optic disc and viewed on a frozen reference infrared fundus image. This enables improved

centering of the optic disc while scanning along the second outer ring of the target area (Figure 2).

We have then addressed the question of whether the examination must be performed in dilated eyes or if undilated eyes would still deliver reproducible data, as all previous, conventional TD-OCT studies in patients with glaucoma or neurodegenerative disorders have been performed in miosis. Moreover, pupil dilation is sometimes refused in a number of MS patients as to avoid a further impairment of gait disturbances or in order to reduce their fitness to drive as a result of blurred vision. [14] We also investigated whether or not the ART- mode would need to be permanently activated or if reacquisition of each OCT image with consecutive repositioning of the target area over the optic disc would be more accurate. We found that in direct comparison, the RNFLT measurements did not significantly differ when calculated in dilated or undilated eyes. We also found that - at least for clear optic media - the HS mode would be equivalent to the HR mode, regarding the image acquisition under conveniently undilated pupil conditions. In severely opaque ocular media, however, this may not hold true, as in such cases a HR image may be needed to gain a reliably segmentable image (Figure 3). [15]

As many neurodegenerative diseases constitute chronically progressive disorders, tight follow-up visits are often required to monitor disease progression accurately. Thus, it is important to assess the variability of RNFLT measurements between consecutive follow-up visits. [16, 17] For the detection of changes during follow-up, however, it is further crucial to obtain a high quality reliable baseline examination. The registered baseline examination can be stored in the device. For this purpose, any obtained follow-up examinations will be directly compared to the first examination by digitally referencing the initial image (e.g. exactly lining up the OCT circle scan around the optic nerve). Additionally, the OCT software can identify previous scan locations and "guide" the OCT broadband light source to scan the same location repeatedly, thereby enabling, for the first time, a true follow-up measurement while still reducing movement artifacts.

In this study, our results showed agreement between consecutive follow-up measurements independent of the acquisition mode (Table 2). Consecutive follow-up scanning of identical peripapillary RNFL locations (referring to defined baseline scans) demonstrates low intersession variability. Thus, this technology provides follow-up examinations independent of the examiner. [18, 19] Intrasession comparison at baseline however, produces slightly higher COVs (Table 1), as this reflects data taken from three independent measurements without activated follow-up mode.

It must be noted that image scan acquisition by eye tracking and activated ART mode only produces higher COVs at baseline. The clue for reducing the COV thus seem to utilize the follow-up function in parallel with activated ART-mode and TrueTrac™ function.

This is a major difference in the concept of image acquisition between eye-tracking guided SD-OCT scanning and other conventional or high-resolution OCT models that perform sweep scans. Here, a large defined area around the optic disc is scanned in the shortest time, without correcting for eye movements. Decentering and image artifacts during the scanning process and decreased reproducibility of retinal thickness measurements are noted over time. Peripapillary scans may as such increasingly differ from visit to visit. [18]

Hence, the high level of reproducibility of retinal thickness measurements with the SD-OCT in healthy subjects can be clearly attributed to 1) a combination of optimized disc centering due to the „locking“ of an image during the activated ART-mode as well as the integrated correction for eye movements with the TruTrack™ eye tracking capability during the scanning process at baseline; 2) the implementation of a true follow-up scanning of identical RNFL locations at each follow-up visit; and 3) sophisticated retinal segmentation algorithms providing comparable results both under fast (HS) and high-quality image (HR) acquisition conditions, independent of the pupil width.

Interestingly, the highest COV was found in the thinnest (temporal) sectors, which has the smallest mean and hence the

smallest denominator in the COV equation. Whilst not statistically significant, it might still be clinically relevant.

This would be of much interest in neurodegenerative disorders (e.g. MS, glaucoma) where only subtle changes below the axial resolution could be expected, as the axial resolution of the device is somewhat limited to approximately $7\mu\text{m}$ [20]. Thus, the "technical component of the error" is fixed in terms of micrometers, regardless on how thick the RNFL is. In the consequence this would mean that the COV in atrophy-affected RNFL would be clearly higher, and would hamper a follow-up capacity in diseased eye. However, long-term longitudinal studies would therefore give more relevance to this technology.

In conclusion, the high level of agreement together with the possibility of utilizing a true follow-up measurement confirm the fact that the presented SD-OCT is a promising technology in terms of identifying localized structural damage, e.g. axonal damage. Scanning identical peripapillary regions may enable clinicians to detect discrete levels of retinal thickness changes over time. This is a crucial condition and a prerequisite for the monitoring of neurodegenerative disorders, including (early) glaucoma. Nevertheless, it remains to be evaluated whether peripapillary SD-OCT analysis can provide enough evidence to follow subtle RNFLT changes in short term.

References

1. Lee, J.R., J.W. Jeoung, J. Choi, et al. Structure-Function Relationships in Normal and Glaucomatous Eyes Determined by Time Domain and Spectral Domain Optical Coherence Tomography. *Invest Ophthalmol Vis Sci.* 2010
2. Talman, L.S., E.R. Bisker, D.J. Sackel, et al. Longitudinal study of vision and retinal nerve fiber layer thickness in multiple sclerosis. *Ann Neurol.* 2010; 67: 749-60.
3. Garcia-Martin, E., V. Pueyo, J. Martin, et al. Progressive changes in the retinal nerve fiber layer in patients with multiple sclerosis. *Eur J Ophthalmol.* 2010; 20: 167-73.
4. Fisher, J.B., D.A. Jacobs, C.E. Markowitz, et al. Relation of visual function to retinal nerve fiber layer thickness in multiple sclerosis. *Ophthalmology.* 2006; 113: 324-32.
5. Gordon-Lipkin, E., B. Chodkowski, D.S. Reich, et al. Retinal nerve fiber layer is associated with brain atrophy in multiple sclerosis. *Neurology.* 2007; 69: 1603-9.
6. Wojtkowski, M., V. Srinivasan, J.G. Fujimoto, et al. Three-dimensional retinal imaging with high-speed ultrahigh-resolution optical coherence tomography. *Ophthalmology.* 2005; 112: 1734-46.
7. Cettomai, D., M. Pulicken, E. Gordon-Lipkin, et al. Reproducibility of optical coherence tomography in multiple sclerosis. *Arch Neurol.* 2008; 65: 1218-22.
8. Wolf-Schnurrbusch, U.E., V. Enzmann, C.K. Brinkmann, et al. Morphologic changes in patients with geographic atrophy assessed with a novel spectral OCT-SLO combination. *Invest Ophthalmol Vis Sci.* 2008; 49: 3095-9.
9. Cheung, C.Y., C.K. Leung, D. Lin, et al. Relationship between retinal nerve fiber layer measurement and signal strength in optical coherence tomography. *Ophthalmology.* 2008; 115: 1347-51, 1351 e1-2.
10. Wu, Z., J. Huang, L. Dustin, et al. Signal strength is an important determinant of accuracy of nerve fiber layer thickness measurement by optical coherence tomography. *J Glaucoma.* 2009; 18: 213-6.
11. Sergott, R.C., E. Frohman, R. Glanzman, et al. The role of optical coherence tomography in multiple sclerosis: expert panel consensus. *J Neurol Sci.* 2007; 263: 3-14.
12. Costello, F., W. Hodge, Y.I. Pan, et al. Differences in retinal nerve fiber layer atrophy between multiple sclerosis subtypes. *J Neurol Sci.* 2009
13. Menke, M.N., G.T. Fekke, and C.L. Trempe. OCT measurements in patients with optic disc edema. *Invest Ophthalmol Vis Sci.* 2005; 46: 3807-11.
14. Vizzeri, G., C. Bowd, F.A. Medeiros, et al. Effect of improper scan alignment on retinal nerve fiber layer thickness measurements using Stratus optical coherence tomograph. *J Glaucoma.* 2008; 17: 341-9.
15. Pierre-Kahn, V., R. Tadayoni, B. Haouchine, et al. Comparison of optical coherence tomography models OCT1 and Stratus OCT for macular retinal thickness measurement. *Br J Ophthalmol.* 2005; 89: 1581-5.
16. Budenz, D.L., R.T. Chang, X. Huang, et al. Reproducibility of retinal nerve fiber thickness measurements using the stratus OCT in normal and glaucomatous eyes. *Invest Ophthalmol Vis Sci.* 2005; 46: 2440-3.
17. Paunescu, L.A., J.S. Schuman, L.L. Price, et al. Reproducibility of nerve fiber thickness, macular thickness, and optic nerve head measurements using StratusOCT. *Invest Ophthalmol Vis Sci.* 2004; 45: 1716-24.
18. Wu, Z., M. Vazeen, R. Varma, et al. Factors associated with variability in retinal nerve fiber layer thickness measurements obtained by optical coherence tomography. *Ophthalmology.* 2007; 114: 1505-12.

19. Mwanza, J.C., R.T. Chang, D.L. Budenz, et al. Reproducibility of Peripapillary Retinal Nerve Fiber Layer Thickness and Optic Nerve Head Parameters Measured with Cirrus™ HD-OCT in Glaucomatous Eyes. *Invest Ophthalmol Vis Sci.* 2010
20. Henderson, A.P., S.A. Trip, P.G. Schlottmann, et al. A preliminary longitudinal study of the retinal nerve fiber layer in progressive multiple sclerosis. *J Neurol.* 2010; 257: 1083-91.

Figure legends

Figure 1. Comparison of the RNFLT measurements (μm) using a baseline examination and two consecutive follow-up measurements. No statistically significant differences were detected. This was independent of the measurement of the RNFLT at baseline (base), first (F1) or second (F2) follow-up visit, as well as the peripapillary sector examined. This was examined in an averaged RNFLT (G) or split into the four sectors (temporal, inferior, nasal and superior). The results are plotted using box-plots.

Figure 2. Exact centering of the peripapillary scan is essential for reproducible data. (A) shows a slightly decentered, peripapillary scan. The RNFLT measurements are different from the (B) centered scan. Additionally the software-based internal control misclassifies the temporal scan as pathological (red segment).

Figure 3. Detection of the RNFLT in opaque media. In opaque media (in this case a left eye with a cortical cataract) the automatic segmentation of the RNFLT fails altogether (A) in the first place. Upon several tries the segmentation is somewhat successful, however it underestimates the RNFLT, in the case of detection using the HS mode (B). In HR mode (C) the RNFLT is successfully detected.

Table 1. Baseline comparison of RNFLT measurements (μm) around the optic nerve either globally (G), temporal (temp), inferior (inf), nasal (nas) or superior (sup). The modes used were undilated (Mi), dilated (My), High Resolution (HR), High Speed (HS). Usage of the locked ART mode is indicated with -A. We calculated the mean, standard deviation (stdev) and the intrasession coefficient of variation (COV) from the data described. We show, in all conditions, low COV between 0.55% (G, My-HS-A) and 3.97% (temp, My-HR). The highest COVs were detected in the temporal sector ranging between 2.71% (Mi-HS-A) and 3.97% (My-HR).

Table 2. Follow-up-comparison of RNFLT measurements (μm) over three different days around the optic nerve either globally (G), temporal (temp), inferior (inf), nasal (nas) or superior (sup). The data are shown in regard to a baseline examination and two consecutive examinations under identical conditions on the two following days (F1 and F2). Again we calculated the mean, standard deviation (stdev) and the intersession COV using the different conditions described previously (all examinations have been performed in undilated (Mi) and dilated (My) eyes using either high resolution (HR) or high speed (HS) modes).

Figure 1

a



Figure 2

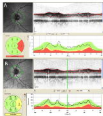


Figure 3

